ACCELERATED COMMUNICATION

Privileged Access to Mitochondria of Calcium Influx through N-Methyl-D-Aspartate Receptors

TSUNG-I PENG and J. TIMOTHY GREENAMYRE

Departments of Neurology (T.-I.P., J.T.G.) and Pharmacology (J.T.G.) and the Wesley Woods Laboratory for Brain Sciences (T.-I.P., J.T.G.), Emory University School of Medicine, Atlanta, Georgia 30322

This paper is available online at http://www.molpharm.org

ABSTRACT

Mitochondrial Ca^{2+} uptake responds dynamically and sensitively to changes in cytosolic Ca^{2+} levels and plays a crucial role in sequestering the large Ca^{2+} load induced by N-methyl-D-aspartate (NMDA) receptor activation. However, the precise interrelationships between NMDA receptor activation, cytosolic Ca^{2+} increase, and mitochondrial Ca^{2+} uptake remain obscure. To reliably, independently, and simultaneously detect cytosolic and mitochondrial Ca^{2+} concentration changes in the same cell, we loaded primary striatal neurons with two Ca^{2+} indicators, calcium green 1N and rhod-2, and visualized the fluorescence signals from single neurons with laser scanning confocal fluorescence microscopy. In kinetic data analysis, only calcium green signals from predefined cytosolic areas and rhod-2 signals from predefined mitochondrial regions were used, and attention was focused on the initial rapid rising phase of the responses. When neurons were treated with 100 μM NMDA, increases of cytosolic and mitochondrial Ca^{2+} showed similar time courses and rates of change, and seemed to be time-locked. In contrast, when neurons were treated with 100 μM kainate, 50 mM KCl, or 0.3 μM ionomycin, mitochondrial Ca^{2+} increases lagged behind cytosolic Ca^{2+} increases. These data suggest that mitochondrial Ca^{2+} uptake in response to an increase of cytosolic Ca^{2+} is faster and more tightly coupled during NMDA receptor activation than during non-NMDA receptor or voltage-dependent Ca^{2+} channel activation. This proficient mitochondrial Ca^{2+} uptake may avert a large rise in cytosolic Ca^{2+} concentration in response to NMDA receptor activation. Yet, it may lead to excessive Ca^{2+} accumulation inside mitochondria and render mitochondria susceptible to Ca^{2+} mediated injury.

Massive Ca^{2+} influx through NMDA receptor channels may be the primary mediator triggering glutamate-induced neuronal death. Neurons survive when challenged by NMDA in the absence of extracellular Ca^{2+} or in the presence of intracellular Ca^{2+} chelators (Choi, 1987; Tymianski *et al.*, 1993); and the severity of glutamate neurotoxicity depends on the transmembrane Ca^{2+} gradient (Tymianski *et al.*, 1993). A large rise in $[Ca^{2+}]_i$ resulting from Ca^{2+} influx, however, may not in itself be the primary determinant of subsequent cell death, and all Ca^{2+} influxes may not be equally neurotoxic (Tymianski *et al.*, 1993). Studies using high affinity fluorescent Ca^{2+} indicators (e.g., Fura-2, Indo-1) to measure $[Ca^{2+}]_i$ do not show a correlation between the magnitude of glutamate-induced $[Ca^{2+}]_i$ increase and degree of neurotoxicity (Tymianski *et al.*, 1993; Wang and Thayer, 1996). Wang and Thayer (1996) showed that the amplitude of the glutamate-induced $[Ca^{2+}]_i$ increase reached a maximum at 30 μM glutamate, a nontoxic concentration with 5 min exposure, whereas maximal neurotoxicity was elicited at glutamate concentrations > 300 μM. Large rises in $[Ca^{2+}]_i$ evoked by non-NMDA glutamate receptor activation or by voltage-gated Ca^{2+} channels that were of equal magnitude to those induced by NMDA receptor activation did not result in extensive neuronal death (Tymianski *et al.*, 1993). Hartley *et al.* (1993) and Eimerl and Schramm (1994) showed that glutamate-induced neurotoxicity correlates with Ca^{2+} load measured by $^{45}Ca^{2+}$ uptake, but not with $[Ca^{2+}]_i$ measured by Fura-2. The total amount of $^{45}Ca^{2+}$ taken up into cultured cerebellar neurons during toxic NMDA receptor ac-

ABBREVIATIONS: NMDA, N-methyl-D-aspartate; FBS, fetal bovine serum; DMEM, Dulbecco's modified Eagle's medium; HEPES, 4-(2-hydroxyethyl)-1-piperazineethanesulfonic acid; $[Ca]_i$, intracellular free calcium concentration; $[Ca]_c$, cystolic calcium concentration; $[Ca]_m$, mitochondrial calcium concentration; AM, acetoxymethyl.

tivation is about 17 mM, which is 10,000 times the maximal measured [Ca^{2+}]$_i$. These data suggest that most of the Ca^{2+} taken up through the NMDA receptor is probably sequestered by subcellular organelles. The only organelle capable of accumulating such massive amounts of Ca^{2+} is the mitochondrion.

In addition to serving as the neuron's primary source of energy, mitochondria act as important buffers of cytosolic Ca^{2+} (Werth and Thayer, 1994) and help to prevent excessive, prolonged elevation of [Ca^{2+}]$_i$. The huge electrochemical proton gradient across the inner mitochondrial membrane, generated by active extrusion of protons along the electron transport chain, provides a strong driving force for Ca^{2+} uptake through a Ca^{2+}-selective uniporter. Mitochondrial Ca^{2+} uptake is sensitive to physiological changes in [Ca^{2+}]$_i$, is rapid and reversible, and has a huge capacity (Sparagna *et al.*, 1995; Jou *et al.*, 1996; Trollinger *et al.*, 1997; Babcock *et al.*, 1997). Inhibitors that disrupt mitochondrial Ca^{2+} uptake severely compromise clearance of cytosolic Ca^{2+} after an imposed elevation (White and Reynolds 1995, 1997; Wang and Thayer 1996), leading to a huge increase in peak [Ca^{2+}]$_i$ and prolonged recovery time to base-line. Several studies indicate that mitochondrial Ca^{2+} uptake plays a prominent role in buffering the large Ca^{2+} load induced by intense glutamate receptor stimulation, and Ca^{2+} entry into mitochondria may account for the poor correlation between glutamate-induced neurotoxicity and glutamate-induced changes in [Ca^{2+}]$_i$ (Wang and Thayer 1996; White and Reynolds 1995, 1997; Khodorov *et al.*, 1996).

Excessive Ca^{2+} influx into mitochondria may result in mitochondrial dysfunction (Schinder *et al.*, 1996). Prominent, sustained mitochondrial depolarization follows intense NMDA receptor stimulation, and closely parallels the incidence of neuronal death (Schinder *et al.*, 1996; White and Reynolds, 1996). Impaired ATP production (Wang *et al.*, 1994), increased generation of reactive oxygen species (Coyle and Puttfarcken, 1993), and other detrimental processes (e.g., opening of the permeability transitional pore) have also been suggested to result from Ca^{2+}-mediated mitochondrial injury after NMDA receptor stimulation. Substantial Ca^{2+} can be accumulated in mitochondria as a result of overloading the matrix with Ca^{2+}; this disrupts the structural and functional integrity of the organelle (Garthwaite and Garthwaite, 1986). Hence, mitochondria may be critical intracellular targets of injury after intense NMDA receptor stimulation (White and Reynold, 1996) and, in this way, may act as a plausible link between massive Ca^{2+} influx and glutamate neurotoxicity (Schinder *et al.*, 1996).

Still, the unique relationships between NMDA receptor activation, cytosolic Ca^{2+} fluxes, and mitochondrial Ca^{2+} uptake remain obscure. Do mitochondria take up Ca^{2+} at the same rate, regardless of which cytosolic Ca^{2+} influx pathway is activated? To explore this question, we loaded cultured striatal neurons with two fluorescent Ca^{2+} indicators, calcium green and rhod-2, to independently and simultaneously monitor cytosolic and mitochondrial Ca^{2+} changes in the same cell. After challenges with NMDA, kainate, KCl, or ionomycin, we examined and compared cytosolic and mitochondrial Ca^{2+} transients to determine the selectivity of mitochondrial Ca^{2+} uptake in response to different sources of cytosolic Ca^{2+} influx. Our results suggest that Ca^{2+} entering

through NMDA receptors has "privileged" access to mitochondria.

Materials and Methods

Primary striatal neuronal culture. Striata from brains of Sprague-Dawley rat pups on embryonic day 17 were dissected and dissociated as described previously (Peng *et al.* 1998). Dissociated cells were plated onto 25-mm round glass coverslips (no. 1) precoated with poly-D-lysine (0.5 mg/ml, overnight) at a density of 110,000 cells per coverslip and maintained in 10% FBS/DMEM media in the incubator with 5% CO$_2$ at 37°. To enhance the survival rate of this low density neuronal culture, coverslips plated with confluent glial cells were inverted and placed above the coverslips plated with neurons. In this bilaminar system, the two coverslips were separated by wax pegs so as not to have any direct contact between the two coverslips. Two days after plating, cells were treated with 2 mM cytosine arabinoside (Ara-C) in 2.5% FBS/N2/DMEM medium (DMEM media with 2.5% FBS and 10% N2.1 nutrient) for the next 2 days to inhibit the growth of astrocytes. The culture media was then replaced by serum-free N2/DMEM medium. Neurons were maintained in this medium for up to 16 days in culture. The neurons employed for experiments were generally cultured for 9–12 days.

Fluorescent Ca^{2+} indicator loading. Glass coverslips with striatal neurons were rinsed with HEPES-buffered salt solution (containing 140 mM NaCl, 5.4 mM KCl, 1.8 mM CaCl$_2$, 0.8 mM MgCl$_2$, 10 mM glucose, 10 mM HEPES, pH 7.4), then incubated in buffer solution containing 2 μM rhod-2/AM (Molecular Probes, Eugene, OR) at 25° for 6–10 min. Coverslips were rinsed again, then reincubated in buffer solution containing 5 μM calcium green 1N/AM (Molecular Probes) at 37° for 40–50 min. The coverslips were rinsed again and maintained at room temperature in the buffer solution for an additional 20 min before the experiment.

Laser scanning confocal microscopy. Glass coverslips with dye-loaded cells were mounted in a perfusion chamber and secured on the stage of a Zeiss Axioskop microscope equipped with the Insight Point laser scanning confocal system (Meridian Instruments). Neurons were sequentially excited by the 488-nm line of an argon laser (for calcium green) and the 568-nm line of a krypton laser (for rhod-2) through a dual band dichroic mirror. The emitted fluorescence signals from single neurons were filtered sequentially through a 530/30-nm band pass filter (for calcium green) and a 605-nm long pass filter (for rhod-2) mounted on a rotating wheel and were detected by an intensified charge-coupled device camera. The confocal pinhole aperture ranged from 80 to 135 μm. A 100× oil immersion objective (1.4 NA) was used in all experiments. The fluorescence signals were digitized and images were stored in random access memory. The time taken to acquire an image ranged from 0.15 to 0.4 sec. Each set of fluorescence images was recorded at a rate of 0.5 Hz. Each neuron studied represents a separate experiment using a separate culture well and coverslip. Control experiments using singly labeled cells demonstrated that our excitation and detection scheme allowed no cross-talk between fluorophore-detection pairings. That is, the calcium green signal was not detected in the rhod-2 channel, and the rhod-2 signal was not detected in the calcium green channel.

Kinetic data analysis. As described previously (Peng *et al.*, 1998), the rhod-2 signal is highly localized in mitochondria, and as described below, the calcium green signal is seen diffusely throughout the cytoplasm. Therefore, to improve the specificity and signal-to-noise ratio of our measurements, calcium green signals from predefined cytosolic areas and rhod-2 signals from predefined mitochondrial areas in single neurons were used for measurement of signal intensity. Fluorescence intensities at a given time point were normalized to base-line values (expressed as F/F_0, where F_0 is the base-line value) and plotted against time. In some experiments, to better compare the time courses of the calcium green and rhod-2 fluorescence intensity changes, fluorescence was normalized and

expressed as a percentage of the maximal increase $[F(\%\text{max}) = ((F - F_{\text{base}})/(F_{\text{peak}} - F_{\text{base}})) \times 100\%]$. These normalized data were fitted to single exponential equations that yielded rate constants (K) from which $t_{1/2}$ values were calculated according to the equation $t_{1/2} = 0.693/K$. The $t_{1/2}$ values were used to compare the rates of increase in fluorescence intensity within and across experiments.

Stimulating agents. NMDA, kainate, and ionomycin (a calcium ionophore), were added in HEPES-buffered salt solution. In the KCl experiment, the HEPES buffer contained 50 mM KCl and 95 mM NaCl, maintaining the original ionic strength and osmolarity.

Statistics. For each stimulus (e.g., NMDA), the $t_{1/2}$ values for cytosolic and mitochondrial Ca^{2+} transients were calculated simultaneously for all replicate experiments by fitting the data to single exponential equations using the Prism software package for Macintosh (GraphPAD Software, San Diego, CA). The fits to the exponential equations of cytosolic versus mitochondrial fluorescence changes for each stimulus were compared by two-tailed t tests. Comparison of fits across experiments (e.g., comparing the cytosolic $t_{1/2}$ for each stimulus) was by analysis of variance with *post hoc* Bonferroni tests.

Results and Discussion

Concurrent imaging of cytosolic and mitochondrial Ca^{2+} with calcium green and rhod-2. Most of the published studies on the role of mitochondria in buffering cytosolic Ca^{2+} loads have employed a single fluorescent Ca^{2+} indicator, such as Fura-2 or Indo-1, to monitor changes in intracellular Ca^{2+} concentration ($[Ca^{2+}]_i$). These Ca^{2+} indicators can easily get into the cell and distribute not only in the cytosol, but also into subcellular organelles, depending on loading temperature and loading time. Changes in the fluorescence signal from these Ca^{2+} indicators in response to Ca^{2+} increases reflect changes in both the cytosol and the organelles into which the indicators have partitioned. In this study, to reliably, independently, and simultaneously detect cytosolic and mitochondrial Ca^{2+} concentration changes in the same cell, we used two fluorescent Ca^{2+} indicators, calcium green and rhod-2. Unlike most fluorescent Ca^{2+} indicators that carry negative charges, rhod-2/AM (cell membrane-permeable form) contains one net positive charge. This unique chemical feature allows it to accumulate selectively into the highly negatively charged mitochondrial matrix. Once inside the matrix, mitochondrial esterases cleave the AM ester to liberate rhod-2 (membrane-impermeable free acid form). However, when loaded at warm temperature (37°), cytosolic esterases are active enough that the AM esters are cleaved before rhod-2/AM can enter mitochondria. This can lead to substantial cytosolic loading (unpublished observations). At cooler loading temperatures, when enzymatic activity is slowed, the fluorophore esters can reach the mitochondria before being hydrolyzed. We loaded rhod-2/AM into striatal neurons at room temperature to favor mitochondrial loading, and used a low concentration of the indicator (1–2 μM), and a short loading time (5–10 min) to minimize cytosolic loading. With this loading technique, we consistently obtain strong mitochondrial rhod-2 signal and weak cytosolic rhod-2 signal (Fig. 1A). We have previously published a more detailed account of the characteristics and selectivity of rhod-2 in monitoring mitochondrial Ca^{2+} concentration changes (Peng *et al.* 1998).

Calcium green loading was performed after rhod-2 loading had completed. The loading condition for calcium green is the reverse of that for rhod-2, i.e., warm loading temperature (37°), high concentration (5 μM), and long loading time (40–50
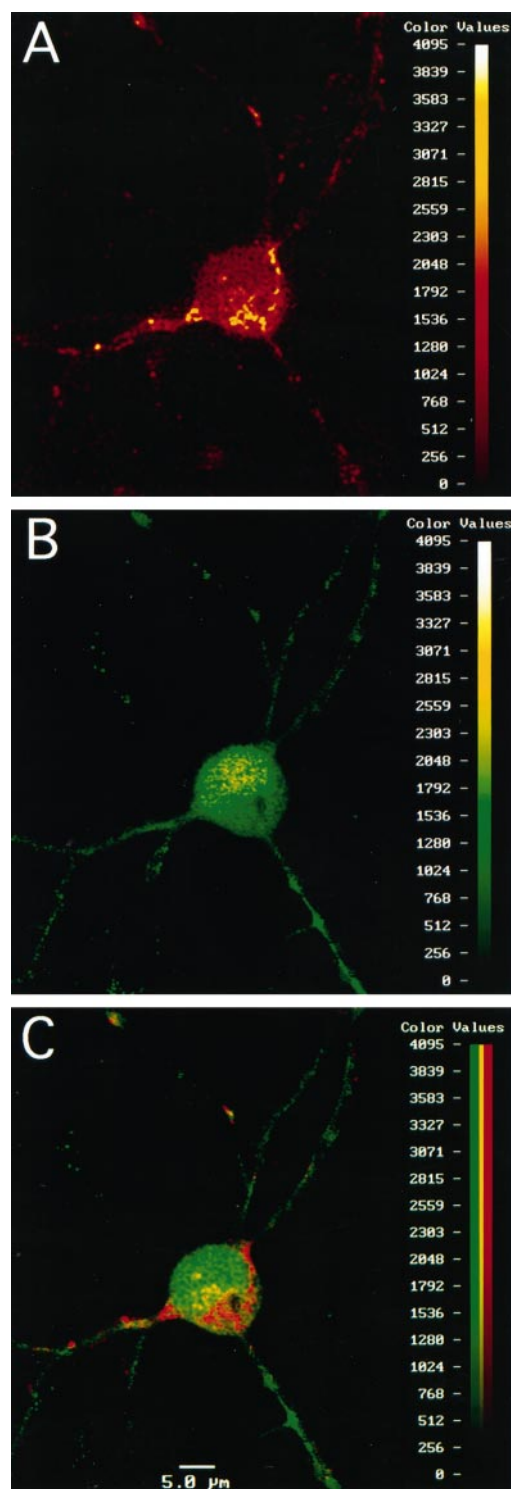

Fig. 1. Confocal fluorescence images of a striatal neuron loaded with two Ca^{2+} indicators, rhod-2 and calcium green. (Refer to Materials and Methods for dye loading procedure and imaging technique.) A, Rhod-2 image. Rhod-2 fluorescence signals reside in highly localized, punctate areas which have been demonstrated to be mitochondria. B, Calcium green image of the same neuron. Calcium green fluorescence signals show a more uniform distribution. C, Superimposed rhod-2 and calcium green images. The intensity of the fluorescence signal is indicated by the *pseudo-color bar* to the *right* in each image. *Scale bar*, 5 μm. In a typical experiment, circular regions of interest, 1–2 μm in diameter, were drawn in a mitochondrial region as defined by high signal in the rhod-2 image (A) and a cytosolic region defined by uniform calcium green signal and lack of rhod-2 signal (e.g., green areas in C). Signal responses from these predefined regions of interest were used to generate the data in this report.

min). Calcium green signal distributes throughout the cell when loaded alone. However, its signal is weaker in mitochondrial areas when loaded after rhod-2 (Fig. 1b). The reasons for this decreased signal in mitochondrial areas are unknown, but unimportant for the present experiments. Instead of detecting the fluorescence signals nonspecifically from the entire cell, as would occur with a microfluorimeter or photomultiplier tube, we imaged the cell with confocal microscopy and measured the calcium green fluorescence intensity in predefined cytosolic areas and the rhod-2 fluorescence intensity in predefined mitochondrial areas. This method avoids unwanted crossover signals between calcium green and rhod-2 in mitochondrial and cytosolic areas, and increases the signal-to-noise ratio when independently monitoring cytosolic and mitochondrial Ca^{2+} concentration changes. Fluorescence images were obtained with brief exposure times (0.15–0.40 sec) at 2-sec intervals to avoid photobleaching and phototoxicity while allowing adequate temporal resolution. In this report, fluorescence intensity changes were not converted into Ca^{2+} concentrations owing to the controversy in using high affinity Ca^{2+} indicators in estimating $[Ca^{2+}]_i$. For example, Hyrc *et al.* (1997) suggested that high affinity Ca^{2+} indicators may underestimate $[Ca^{2+}]_i$, even at levels that seem to be within their range of detection.

Source specificity for fast mitochondrial Ca^{2+} uptake. Previous studies on glutamate- (or NMDA-) induced Ca^{2+} load buffering by mitochondria have focused on changes in the magnitude of the peak $[Ca^{2+}]_i$ transient and the recovery time to base-line $[Ca^{2+}]_i$ levels that result from mitochondrial Ca^{2+} uptake inhibition (White and Reynold, 1995, 1997; Wang and Thayer, 1996; Khodorov *et al.*, 1996). That there is a much greater Ca^{2+} load induced by glutamate compared with KCl-induced membrane depolarization was suggested by the observation that inhibition of mitochondrial Ca^{2+} uptake markedly potentiated the peak $[Ca^{2+}]_i$ and prolonged the recovery time after a glutamate challenge but not after depolarization. In these experiments, the effects of mitochondrial Ca^{2+} uptake inhibition were inferred from changes in $[Ca^{2+}]_i$ measured with a single fluorescence indicator, which primarily reflected cytosolic Ca^{2+} concentration ($[Ca^{2+}]_c$) changes. With this method, $[Ca^{2+}]_m$ changes could not be observed directly.

Using our method to directly, independently, and simultaneously detect mitochondrial and cytosolic Ca^{2+} changes in the same cell, we were interested in studying 1) the time courses of cytosolic and mitochondrial Ca^{2+} transients, and 2) whether mitochondrial Ca^{2+} uptake elicited by NMDA receptor activation is different from that induced by other routes of Ca^{2+} entry. Changes of $[Ca^{2+}]_c$ and $[Ca^{2+}]_m$, as reflected by changes in calcium green and rhod-2 fluorescence from single striatal neurons treated with 100 μM NMDA, 100 μM kainate, or 50 mM KCl are shown in Fig. 2. (Most non-NMDA glutamate receptors have limited Ca^{2+} permeability and we did not perform ion substitution experiments. Therefore, we cannot make firm conclusions as to what proportion of the Ca^{2+} entry elicited by kainate in these experiments was because of secondary activation of voltage-dependent Ca^{2+} channels.) The calcium green and rhod-2 fluorescence intensity changes are overlaid to compare the time courses of the $[Ca^{2+}]_c$ and $[Ca^{2+}]_m$ responses. In the initial rising phase after all three stimuli, both $[Ca^{2+}]_m$ and $[Ca^{2+}]_c$ reached peak levels in less than 30 sec and remained

at those levels in the continued presence of the stimulus. We intentionally scaled the peak F/F_0 values of calcium green and rhod-2 to the same height for better comparison of the time courses. This does not indicate that $[Ca^{2+}]_m$ and $[Ca^{2+}]_c$ are at the same absolute level. In fact, after stimulating chromaffin cells co-loaded with calcium green and rhod-2 with electrical pulses, Babcock *et al.* (1997) estimated that the peak levels of $[Ca^{2+}]_m$ and $[Ca^{2+}]_c$ were different.

In Fig. 2, the $[Ca^{2+}]_c$ recovery time for the NMDA-induced response is longer than those for kainate or KCl, an observation in accordance with what has already been reported by others (White and Reynolds, 1995; Wang and Thayer, 1996).
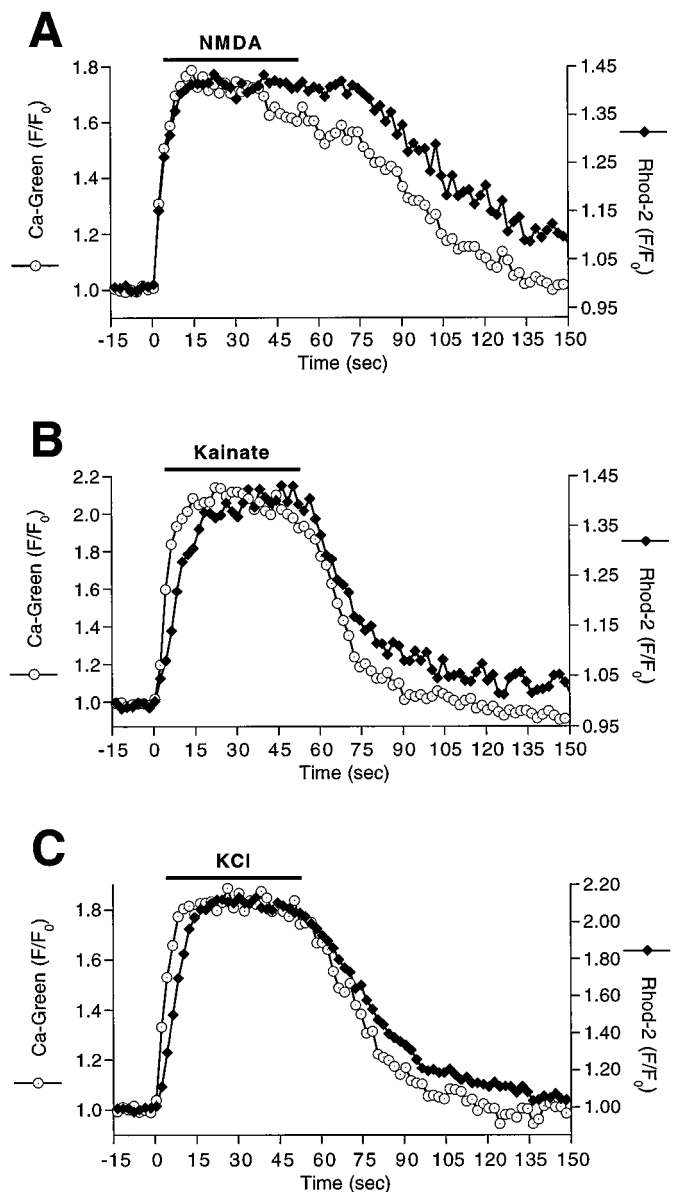

Fig. 2. Simultaneous monitoring of cytosolic and mitochondrial Ca^{2+} transients, as detected by changes in calcium green and rhod-2 fluorescence intensity, in single striatal neurons treated with (A) 100 μM NMDA, (B) 100 μM kainate, or (C) 50 mM KCl. Fluorescence intensity changes were normalized and expressed as F/F_0 values, where F_0 is the fluorescence intensity at base-line. Only one representative experiment from each treatment group is shown. The recovery time to return to base-line levels for NMDA-induced increases in cytosolic and mitochondrial Ca^{2+} are longer than those for kainate or KCl induced responses.

White and Reynolds (1997) noted that the $[Ca^{2+}]_i$ recovery time is correlated with the magnitude of the Ca^{2+} load induced by glutamate, and that the recovery of $[Ca^{2+}]_i$ to baseline after glutamate removal is critically regulated by release of Ca^{2+} from mitochondrial stores. Hence, in the present experiments, the longer $[Ca^{2+}]_c$ recovery time after NMDA application most likely indicates a larger Ca^{2+} load imposed on mitochondria. Interestingly, $[Ca^{2+}]_m$ recovery followed a similar but more prolonged time course than $[Ca^{2+}]_c$ in all cases. This more protracted $[Ca^{2+}]_m$ recovery was also noted by Babcock *et al.* (1997) after electrical depolarization of chromaffin cells. The mechanism and significance of this phenomenon await further investigation.

Although it seems that NMDA receptor activation imposes a larger Ca^{2+} load on mitochondria than other stimuli, the question remains as to whether mitochondria take up Ca^{2+} more efficiently in response to NMDA stimulation relative to other Ca^{2+} influx mechanisms. To address this issue we

focused more closely on the initial rising phase of the Ca^{2+} response elicited by the various agonists. Fig. 3 shows the average changes in cytosolic and mitochondrial fluorescence levels during the first 16 sec after application of 100 μM NMDA, 100 μM kainate, 50 mM KCl, or 0.3 μM ionomycin. Because the maximal F/F_0 values of calcium green and rhod-2 varied from cell to cell across experiments (White and Reynolds, 1997; Peng *et al.*; 1998), fluorescence was normalized, expressed as a percent of the maximal increase, and fitted to exponential equations. The time needed to reach 50% of the maximal increase in fluorescence intensity ($t_{1/2}$) was used to compare the rate of increase in fluorescence intensity across different experiments.

As shown in Figs. 3B and 4, during stimulation with NMDA, the $t_{1/2}$ values of cytosolic and mitochondrial Ca^{2+} accumulation were virtually identical (2.71 ± 0.09 versus 2.89 ± 0.17 sec; $n = 4$; not significant). These data suggest that mitochondrial and cytosolic Ca^{2+} levels are time-locked
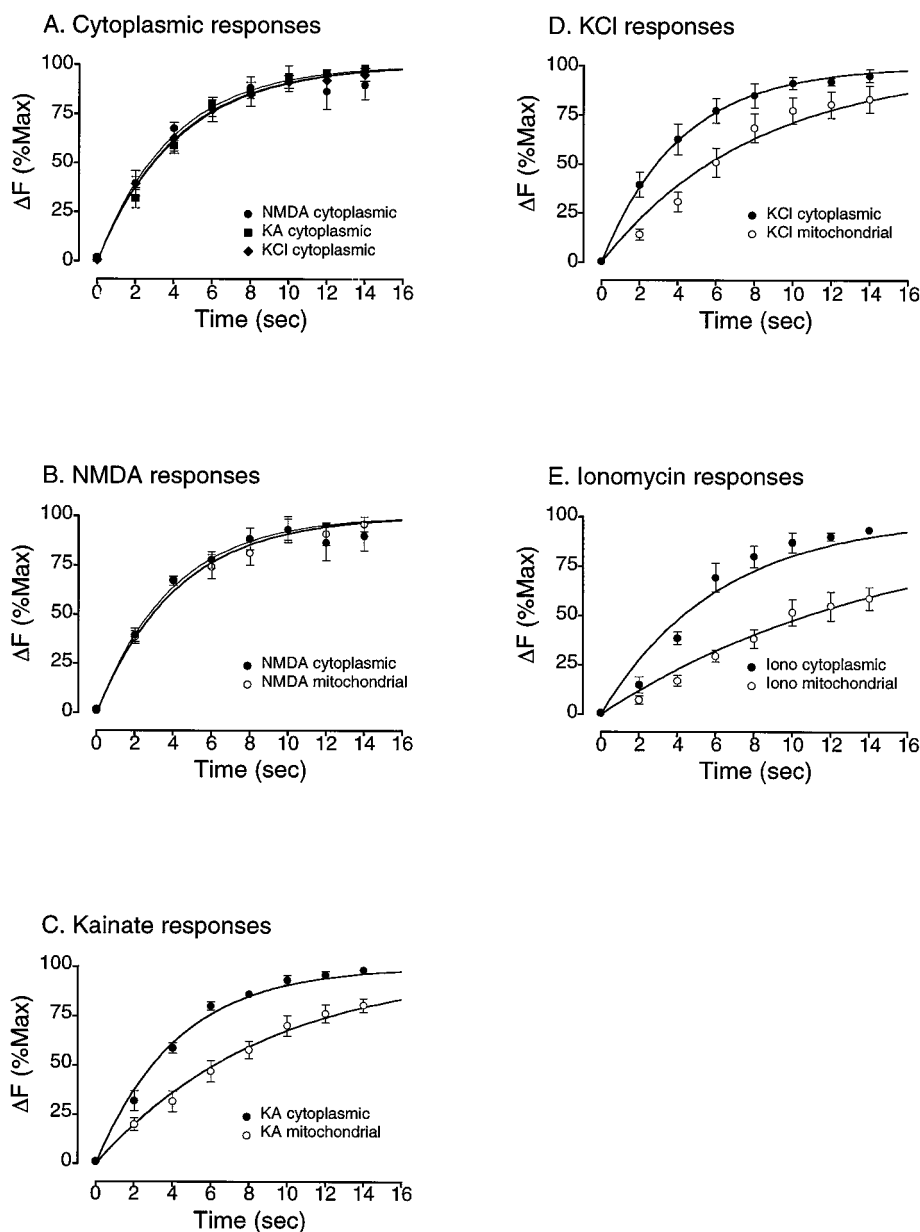

A. Cytoplasmic responses

D. KCl responses

B. NMDA responses

E. Ionomycin responses

C. Kainate responses

Fig. 3. Initial rising phase of the cytosolic and mitochondrial Ca^{2+} responses. Normalized fluorescence data were fitted to exponential curves as described in the text. A, The cytosolic responses to NMDA, kainate and KCl were indistinguishable statistically. B, After NMDA application, the cytosolic and mitochondrial Ca^{2+} transients were virtually identical. C–E, After kainate, KCl, or ionomycin, the mitochondrial response lagged substantially behind the cytosolic response ($p <$ 0.0001). *Points*, mean ± standard error of four independent experiments.

in neurons treated with NMDA. In contrast, mitochondrial Ca^{2+} uptake lagged about 3 sec behind cytosolic Ca^{2+} after kainate stimulation (2.93 ± 0.11 sec versus 6.15 ± 0.25 sec; $n = 4$; $p < 0.0001$) or KCl stimulation (2.86 ± 0.15 sec versus 5.56 ± 0.29 sec; $n = 4$; $p < 0.0001$) (Figs. 3 and 4). The apparently slower mitochondrial Ca^{2+} uptake responses in the kainate and KCl treatment groups are probably not the result of a slower cytosolic Ca^{2+} increase, because 1) the calcium green $t_{1/2}$ values for NMDA, kainate, and KCl were very similar and did not differ statistically from one another (Figs. 3A and 4), and 2) analysis of variance of the mitochondrial $t_{1/2}$ values showed that the mitochondrial response to NMDA was significantly faster than with other stimuli ($p < 0.001$). Note that we did not use lower concentrations of NMDA; therefore, we do not know whether there would be a lag in mitochondrial Ca^{2+} uptake with less intense receptor stimulation. On the other hand, 100 μM is not a saturating concentration of NMDA in terms of receptor activation or neurotoxicity (Verdoorn and Dingledine, 1988; McNamara and Dingledine, 1990), so it is unlikely that the fast mitochondrial Ca^{2+} uptake we observed is because of saturation of the NMDA receptors.

Is fast mitochondrial Ca^{2+} uptake specific to NMDA receptor stimulation? To further address this question, we treated neurons with another type of stimulus, the Ca^{2+} ionophore ionomycin, and determined the kinetics of the mitochondrial Ca^{2+} uptake response. A low dose of ionomycin (0.3 μM) was used in an effort to let Ca^{2+} penetrate the plasma membrane selectively. This ionophore caused a somewhat slower increase in cytosolic Ca^{2+} than the other stimuli (4.27 ± 0.23 sec; $n = 4$), but this did not reach statistical significance. Unlike the NMDA receptor stimulation, the mitochondrial Ca^{2+} uptake response to ionomycin lagged substantially behind the cytosolic response (10.70 ± 0.52 sec; $p < 0.0001$) Together, these data clearly demonstrate that mitochondrial Ca^{2+} uptake induced by NMDA receptor activation is different from that induced by a non-NMDA agonist, voltage-dependent Ca^{2+} channel activation, or a Ca^{2+} ionophore.

Fast mitochondrial Ca^{2+} uptake in response to NMDA receptor activation may have both adaptive and detrimental consequences. Under physiological conditions, rapid mitochondrial Ca^{2+} uptake may act to stimulate mitochondrial

Fig. 4. $t_{1/2}$ values for cytoplasmic and mitochondrial Ca^{2+} transients induced by NMDA, kainate, KCl, and ionomycin. The cytosolic $t_{1/2}$ values for the various stimuli did not differ statistically, nor did the cytosolic and mitochondrial responses to NMDA differ. In contrast, for kainate, KCl, and ionomycin, the mitochondrial $t_{1/2}$ was substantially greater than the corresponding cytosolic response. Error bars, 95% confidence intervals; ***, $p < 0.0001$.

respiration and energy production, and it is well documented that fast mitochondrial Ca^{2+} uptake occurs in other systems. Babcock *et al.* (1997) reported that chromaffin cell mitochondria can take up Ca^{2+} rapidly; more than half of mitochondrial Ca^{2+} uptake is accomplished while cytosolic Ca^{2+} entry elicited by electrical depolarization is still in progress. Trollinger *et al.* (1997) observed rapid mitochondrial free Ca^{2+} transients during each contractile cycle in rhod-2-loaded rabbit cardiac myocytes. The averaged transient showed a half rise time of about 65 msec with a total of 300 msec to rise from base-line to peak fluorescence. These observations demonstrate that mitochondria can rapidly take up *physiological* concentrations of Ca^{2+}. Moreover, fast mitochondrial Ca^{2+} uptake probably helps to prevent a large rise in cytosolic Ca^{2+} after NMDA receptor stimulation, and it helps to shape the $[Ca^{2+}]_i$ response. However, this accelerated mitochondrial Ca^{2+} uptake induced by NMDA may permit excessive mitochondrial Ca^{2+} accumulation and render mitochondria more susceptible to Ca^{2+}-mediated injury. Thus, what is probably a protective mechanism may become a toxic mechanism during excessive or prolonged NMDA receptor activation.

Potential mechanisms. Sparagna *et al.* (1995) demonstrated that Ca^{2+} can be sequestered into mitochondria by two distinct modes, a rapid uptake (high conductivity) mode of very short duration, followed by a slower uptake (low conductivity) mode, which has the characteristics of the uniporter. Could this rapid mode of mitochondrial Ca^{2+} uptake be responsible for the NMDA-induced fast mitochondrial Ca^{2+} uptake observed in this report? If so, why is this rapid uptake mode activated selectively by NMDA but not by kainate or membrane depolarization? Polyamines may provide the answer. Sparagna *et al.* (1995) showed that the rapid mode of mitochondrial Ca^{2+} uptake can be activated specifically by polyamines, especially spermine. Spermine and spermidine are selectively released from striatum by NMDA receptor activation, but not by kainate or quisqualate (Fage *et al.*, 1992). Interestingly, Siddiqui and Iqbal (1994) observed that NMDA receptor-mediated $^{45}Ca^{2+}$ fluxes can be blocked by a polyamine synthesis inhibitor. Porcella *et al.* (1991) and Kish *et al.* (1991) showed that a polyamine synthesis inhibitor is neuroprotective against NMDA-induced brain damage *in vivo*. These observations suggest that the specificity of the NMDA-induced mitochondrial response may be dictated via second messenger activation. In this scenario, activation of NMDA receptors, but not other receptors, may increase local intracellular concentrations of polyamines that would then activate the rapid mode of mitochondrial Ca^{2+} uptake. This possibility is under investigation.

An alternative explanation to be considered is that the NMDA receptor simply allows more calcium to enter the neuron in a shorter period of time than other stimuli. Studies of $^{45}Ca^{2+}$ uptake (Hartley *et al.*, 1993; Eimerl and Schramm, 1994) and experiments using low affinity Ca^{2+} indicators (Hyrc *et al.*, 1997) support this idea. Because the mitochondrial uniporter has a relatively low affinity, it is more efficient at higher cytosolic Ca^{2+} levels. However, this would not seem to be an adequate explanation for the complete lack of a lag phase in NMDA-induced mitochondrial Ca^{2+} uptake. It is also necessary to consider the possibility that mitochondria are simply in closer proximity to NMDA receptors than other routes of Ca^{2+} entry.
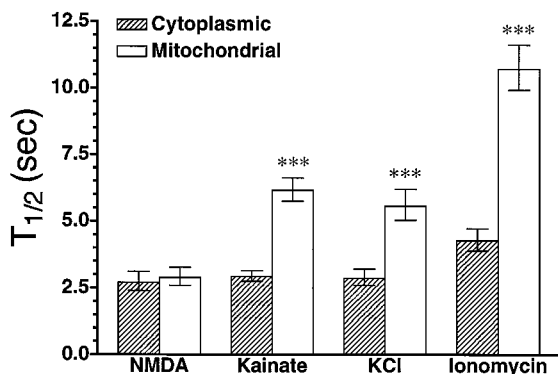
Regardless of the mechanisms, it is clear that Ca^{2+} loads that enter the cytoplasm during NMDA receptor stimulation have more rapid, or "privileged" access to mitochondria. This likely accounts for the selectivity of NMDA receptor activation in producing mitochondrial damage via Ca^{2+}-dependent generation of free radicals and collapse of mitochondrial membrane potential.

Acknowledgments

References

Babcock DF, Herrington J, Goodwin PC, Park YB, and Hille B (1997) Mitochondrial participation in the intracellular Ca^{2+} network. *J Cell Biol* **136:**833–844.

Choi DW (1987) Ionic dependence of glutamate neurotoxicity. *J Neurosci* **7:**369–379.

Coyle JT and Puttfarcken P (1993) Oxidative stress, glutamate, and neurodegenerative disorders. *Science (Washington DC)* **262:**689–695.

Eimerl S and Schramm M (1994) The quantity of calcium that appears to induce neuronal death. *J Neurochem* **62:**1223–1226.

Fage D, Voltz C, Scatton B, and Carter C (1992) Selective release of spermine and spermidine from the rat striatum by *N*-methyl-D-aspartate receptor activation in vivo. *J Neurochem* **58:**2170–2175.

Garthwaite G and Garthwaite J (1986) Amino acid neurotoxicity: Intracellular sites of calcium accumulation associated with the onset of irreversible damage to rat cerebellar neurons in vitro. *Neurosci Lett* **71:**53–58.

Hartley DM, Kurth MC, Bjerkness L, Weiss JH, and Choi DW (1993) Glutamate receptor-induced $^{45}Ca^{2+}$ accumulation in cortical cell culture correlates with subsequent neuronal degeneration. *J Neurosci* **13:**1993–2000.

Hyrc K, Handran SD, Rothman SM, and Goldberg MP (1997) Ionized intracellular calcium concentration predicts excitotoxic neuronal death: Observations with low-affinity fluorescent calcium indicators. *J Neurosci* **17:**6669–6677.

Jou MJ, Peng TI, and Sheu SS (1996) Histamine induces oscillations of mitochondrial free Ca^{2+} concentration in single cultured rat brain astrocytes. *J Physiol (Lond)* **497:**299–308.

Khodorov B, Pinelis V, Storozhevykh T, Vergun O, and Vinskaya N (1996) Dominant role of mitochondria in protection against a delayed neuronal Ca^{2+} overload induced by endogenous excitatory amino acids following a glutamate pulse. *FEBS Lett* **393:**135–138.

Kish SJ, Wilson JM, and Fletcher PJ (1991) The polyamine synthesis inhibitor α-difluoromethylornithine is neuroprotective against *N*-methyl-D-aspartate-induced brain damage in vivo. *Eur J Pharmacol* **209:**101–103.

McNamara D and Dingledine R (1990) Dual effect of glycine on NMDA-induced neurotoxicity in rat cortical cultures. *J Neurosci* **10:**3970–3976.

Peng TI, Jou MJ, Sheu SS, and Greenamyre JT (1998) Visualization of NMDA receptor-induced mitochondrial calcium accumulation in striatal neurons. *Exp Neurol* **149:**1–12.

Porcella A, Fage D, Voltz C, Carter C, Scatton B, and Bartholini G (1991) Difluomethyl ornithine protects against the neurotoxic effects of intrastriatally administered *N*-methyl-D-aspartate in vivo. *Eur J Pharmacol* **199:**267–269.

Schinder AF, Olson EC, Spitzer NC, and Montal M (1996) Mitochondrial dysfunction is a primary event in glutamate neurotoxicity. *J Neurosci* **16:**6125–6133.

Siddiqui F and Iqbal Z (1994) Regulation of *N*-methyl-D-aspartate receptor-mediated calcium transport and norepinephrine release in rat hippocampus synaptosomes by polyamines. *Neurochem Res* **19:**1421–1429.

Sparagna GC, Gunter KK, Sheu SS, and Gunter TE (1995) Mitochondrial calcium uptake from physiological-type pulses of calcium. *J Biol Chem* **270:**27510–27515.

Trollinger DR, Cascio WE, and Lemasters JT (1997) Selective loading of rhod-2 into mitochondria shows mitochondrial Ca^{2+} transients during the contractile cycle in adult rabbit cardiac myocytes. *Biochem Biophys Res Commun* **236:**738–742.

Tymianski M, Charlton MP, Carlen PL, and Tator CH (1993) Source specificity of early calcium neurotoxicity in cultured embryonic spinal neurons. *J Neurosci* **13:**2085–2104.

Verdoorn TA and Dingledine R (1988) Excitatory amino acid receptors expressed in *Xenopus* oocytes: Agonist pharmacology. *Mol Pharmacol* **34:**298–307.

Wang GJ, Randall RD, and Thayer SA (1994) Glutamate-induced intracellular acidification of cultured hippocampal neurons demonstrates altered energy metabolism resulting from Ca^{2+} loads. *J Neurophysiol* **72:**2563–2569.

Wang GJ and Thayer SA (1996) Sequestration of glutamate-induced Ca^{2+} loads by mitochondria in cultured rat hippocampal neurons. *J Neurophysiol* **76:**1611–1621.

Werth JL and Thayer SA (1994) Mitochondria buffer physiological calcium loads in cultured rat dorsal root ganglion neurons. *J Neurosci* **14:**348–356.

White RJ and Reynolds IJ (1995) Mitochondria and Na^+/Ca^{2+} exchange buffer glutamate-induced calcium loads in cultured cortical neurons. *J Neurosci* **15:**1318–1328.

White RJ and Reynolds IJ (1996) Mitochondrial depolarization in glutamate-stimulated neurons: an early signal specific to excitotoxin exposure. *J Neurosci* **16:**5688–5697.

White RJ and Reynolds IJ (1997) Mitochondria accumulate Ca^{2+} following intense glutamate stimulation of cultured rat forebrain neurons. *J Physiol (Lond)* **498**(Pt 1):31–47

Send reprint requests to: Dr. Tsung-I Peng, Department of Neurology, Emory University, 1639 Pierce Drive, WMB 6000, Atlanta, GA 30322.